Article

Thermal Properties and Temporal Dynamics of Red Latosol (Oxisol) in Sustainable Agriculture and Environmental Conservation

Rodrigo Aparecido Jordan [1], Rodrigo Couto Santos [1,*], Ricardo Lordelo Freitas [2], Anamari Viegas de Araújo Motomiya [1], Luciano Oliveira Geisenhoff [1], Arthur Carniato Sanches [1], Hélio Ávalo [1], Marcio Mesquita [3], Maria Beatriz Ferreira [4], Patrícia Costa Silva [5], Ítalo Sabião Sanches [2], Édipo Sabião Sanches [2], Jhon Lennon Bezerra Da Silva [6] and Marcos Vinícius da Silva [7,*]

[1] Faculty of Agricultural Sciences, Federal University of Grande Dourados (FCA/UFGD), Rua João Rosa Góes, 1761—Vila Progresso, Dourados 79825-070, MS, Brazil; rodrigojordan@ufgd.edu.br (R.A.J.); anamarimotomiya@ufgd.edu.br (A.V.d.A.M.); lucianogeisenhoff@ufgd.edu.br (L.O.G.); arthursanches@ufgd.edu.br (A.C.S.); helioavalo@hotmail.com (H.Á.)

[2] Postgraduate Program in Agricultural Engineering, Federal University of Grande Dourados (PPGEA/UFGD), Dourados 78825-070, MS, Brazil; ricardolordelo@hotmail.com (R.L.F.); italosabiao@gmail.com (Í.S.S.); ediposabiao@gmail.com (É.S.S.)

[3] Department of Agronomy, Federal University of Goiás (UFG), Esperança Avenue, Goiânia 74690-900, GO, Brazil; marcio.mesquita@ufg.br

[4] Department of Forest Science, Federal Rural University of Pernambuco (UFRPE), Recife 52171-900, PE, Brazil; beatriz.177@outlook.com

[5] University Unit of Santa Helena de Goiás, Department of Agricultural Engineering, Southwest Campus, State University of Goiás (UEG), Via Protestato Joaquim Bueno, 945, Santa Helena de Goiás 75920-000, GO, Brazil; patricia.costa@ueg.br

[6] Center for Information Management and Science Popularization, National Institute of the Semiarid (INSA), Campina Grande 58434-700, PB, Brazil; jhon.lennon@insa.gov.br

[7] Department of Agricultural Engineering, Federal Rural University of Pernambuco (UFRPE), Rua Dom Manoel de Medeiros, SN, Dois Irmãos, Recife 52171-900, PE, Brazil

* Correspondence: rodrigocouto@ufgd.edu.br (R.C.S.); marcolino_114@hotmail.com (M.V.d.S.)

Abstract: Understanding and characterizing the relationship between soil and environmental temperatures is crucial for developing effective agricultural management strategies, promoting natural resource conservation, and developing sustainable production systems. Despite the direct impact of the thermal properties of Oxisols on global food production and sustainable agriculture, there is a dearth of research in this area. Therefore, this study aimed to monitor and analyze the thermal behavior of a Red Latosol (Oxisol) in Dracena-SP, Brazil, over two years (from 28 July 2020 to 27 July 2022). Using R software (version 4.3.0) and paired group comparisons, we organized the data into twelve-month sets to estimate monthly soil thermal diffusivity using amplitude, arctangent, and logarithm methods. Soil depth and thermal amplitude showed a temporal pattern characterized by inversely proportional magnitudes that followed an exponential behavior. The thermal amplitude of the Oxisol evaluated decreased with increasing depth, indicating soil thermal damping. In conclusion, the relationship between Oxisol and environmental temperature has significant implications for achieving sustainable agriculture and efficient water and plant resource management.

Keywords: analytical methods; sustainable agriculture; thermal amplitude; thermal damping; soil temperature

1. Introduction

Oxisols are one of the primary soil types found in Brazil, which ranks among the world's largest agricultural producers [1,2]. Due to their unique characteristics, these soils present challenges for more sustainable management. As a result, understanding the

intrinsic properties of Oxisols is crucial for achieving sustainable agricultural practices, ensuring food security, and preserving the environment on a global scale [3].

Soil temperature is considered one of the key factors for plant development, directly influencing seed germination, root development and activity, growth rate and duration, and ultimately the quality and quantity of agricultural production [4,5]. Thermal gradients created by daily and seasonal temperature variations at the soil-atmosphere interface drive heat flux within the soil profile [6,7]. The temperature of surface layers is generally strongly affected by these environmental thermal fluctuations, with attenuation occurring at greater depths.

Studying soil thermal conductivity remains a considerable challenge due to its significant spatial and temporal variability, requiring innovative approaches for accurate characterization [8]. New methodologies have actively been developed to improve both field and laboratory measurement techniques. Their main goals are to improve accuracy and the understanding of thermal interactions within the soil environment [9]. As part of these new methodologies, advanced methods such as the transient heat flux technique and the hot plane source technique have emerged, offering greater accuracy and reduced humidity influence during measurements [10]. Additionally, remote sensing techniques have shown potential for mapping thermal conductivity on a regional scale [11,12].

Building on this, Ref. [13] highlights the benefits of ongoing developments in computational simulation models, which enable a more accurate representation of complex spatiotemporal variations in soil thermal behavior. They advocate for a combined approach of experimental, analytical, and computational methods for precise soil thermal conductivity characterization across multiple scales.

Frequent monitoring of soil temperature at different depths is instrumental in gaining a better understanding of soil thermal behavior and determining key soil properties, particularly thermal diffusivity. Thermal diffusivity, the ratio of thermal conductivity to volumetric heat capacity, indicates the rate of heat spread through the soil [14,15]. To estimate soil thermal diffusivity, various methods have been proposed [16]. Notably, these analytical methods have emerged as practical alternatives that yield satisfactory results compared to more expensive laboratory procedures that require specialized equipment [17,18].

As soil thermal properties are heavily influenced by soil type, it is essential to study their thermal behavior in various locations. Such research advances the field, which is currently understudied on Brazilian soils [19,20]. Given the scarcity of research on soil thermal conductivity in Brazil, efforts have intensified to gain deeper insights into the processes related to soil temperature and its impacts on ecosystems. In this context, studies like that of [21] play a crucial role, offering comprehensive analyses of soil temperature under different vegetation covers and shedding light on the implications for the chemical, physical, and biological aspects of ecosystems.

Evaluating Oxisols is essential given their widespread presence in the Brazilian cerrado ecosystem. A study by [22], which focused on the Madeira River region—the largest tributary of the Amazon River—underscores this importance. Their study emphasized not only the predominance of Oxisols in the area but also their significance for the regional ecosystem. They also suggest that a deeper understanding of the intrinsic characteristics of Oxisols could help minimize potential impacts.

In another study, Ref. [23] examined how temperature affects soil aggregation in various Brazilian soil types and management systems. They underscored the complexity of soil-climate-management interactions and called for further research, noting the limited quantification of thermal attributes in Brazilian soils.

Similarly, Ref. [24] explored strategies for enhancing the physical quality of degraded Oxisols in Brazil through crop-livestock integration. These authors highlighted the potential of integrated systems to increase soil resilience but pointed out the complexity of physical attributes and the need for further research, particularly regarding important properties such as thermal conductivity.

Moreover, Ref. [25] explored challenges and opportunities in managing tropical soils, especially Oxisols. Their research brought attention to the vulnerability of Oxisols to degra-

dation and offered insights for sustainable management. Additionally, they identified the study of thermal conductivity in Brazilian Oxisols as one of the challenges to be addressed.

This study aimed to monitor and analyze the thermal behavior of an Oxisol over two years as well as determine its thermal diffusivity using analytical methods, contributing valuable information for sustainable agriculture. Key features of this investigation included: analyzing the soil thermal behavior as a function of environmental temperature over a long experimental period; assessing the soil in both summer and winter conditions; exploring the effects of environmental temperature on thermal diffusivity at various depths; and, throughout the experimental period, examining the thermal amplitude in detail across the depth of the studied soil.

2. Materials and Methods

2.1. Experimental Area Description

The data set for this experiment comprises a time series of soil temperature collected every 5 min at depths of 5, 20, 40, 60, 80, and 100 cm. These measurements were averaged daily over the period from 28 July 2020 to 27 July 2022. The study was conducted in the municipality of Dracena-SP, located at a latitude of 21°28′59.0″ S, a longitude of 51°31′57.0″ W, and an altitude of 419 m in the southeast region of Brazil, in the state of São Paulo. The geographic coordinates of the experimental site were recorded with a high-performance and precision Eyes.sys GPS GNSS receiver, with a measurement error within 0.03 m. Figure 1 depicts the spatial location of the study area, highlighting the positions of Brazil within South America, São Paulo State within Brazil, and Dracena City within São Paulo State.
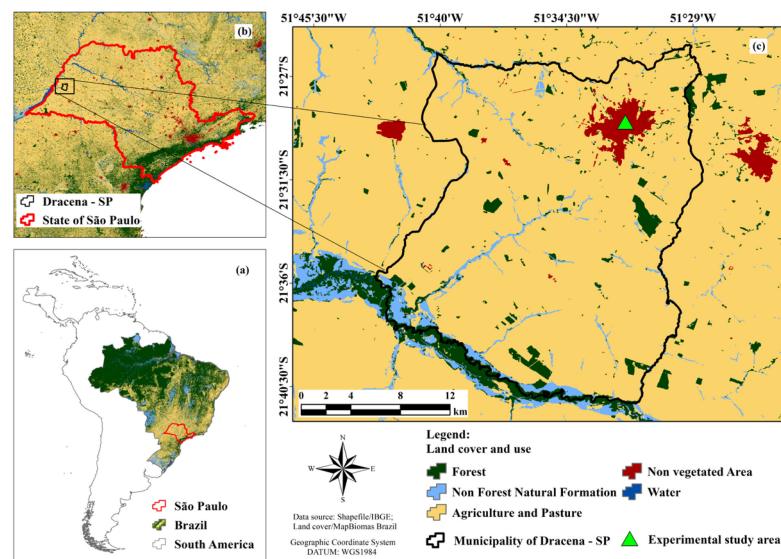

Figure 1. Spatial location of the study area: (**a**) Brazil within South America; (**b**) São Paulo State within Brazil; (**c**) Dracena municipality within São Paulo State.

Dracena has a semi-humid tropical climate, with a rainy summer and a dry winter. The rainy season typically lasts from October to March, with precipitation decreasing from April to September. The region receives an average annual rainfall of 1200 mm, and the average annual temperature ranges from 24 to 26 °C [26]. In the municipality of Dracena, where this study was conducted, Red Latosols (Oxisols) are notably predominant, covering 69.37% of the land [27].

This study was conducted using a single data collection point, as previously developed by [28–30]. This approach is consistent with the findings of [31], who analyzed climatic conditions in Brazil during thermal extremes over 10 years. According to their research, in countries like Brazil with vast territorial areas, it is valid to verify experiments using time series data rather than relying on the spatial distribution of samples.

In this study, the extensive duration of monitoring and meticulous calibration of the sensors ensured repeatable and statistically robust results from single-point sampling. The data were collected over two uninterrupted years, offering solid temporal representativeness.

Subsoil temperature data were obtained at depths of 5, 20, 40, 60, 80, and 100 cm using DS18B20 sensors (Figure 2a), which produce voltage signals proportional to the temperature measured. These data were processed into daily averages. An Arduino Mega 2560 R3 (Figure 2b) collected data at 5-min intervals. We used a Real-Time Clock (RTC) DS3231 Module (Figure 2c) to record date and time and a Micro SD Module (Figure 2d) for data storage.
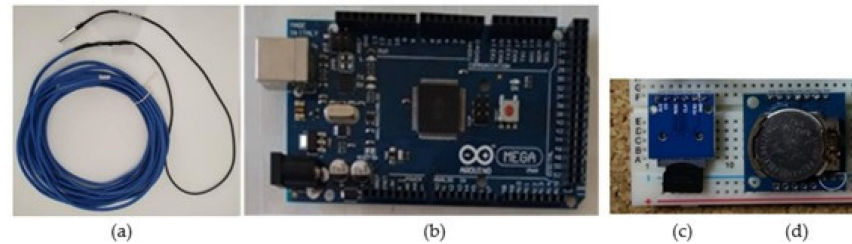

(a)   (b)   (c)   (d)

Figure 2. Equipment used for soil temperature measurement and data recording: (**a**) DS18B20 temperature sensor; (**b**) Arduino Mega 2560 R3; (**c**) Real-Time Clock (RTC) DS3231 Module; and (**d**) Micro SD Module.

The DS18B20 temperature sensors were attached at 20 cm intervals inside a 50-mm-diameter corrugated conduit. This conduit was then inserted into a 3 m long PVC pipe with a 100 mm diameter (Figure 3a) and subsequently placed within the soil (Figure 3b).
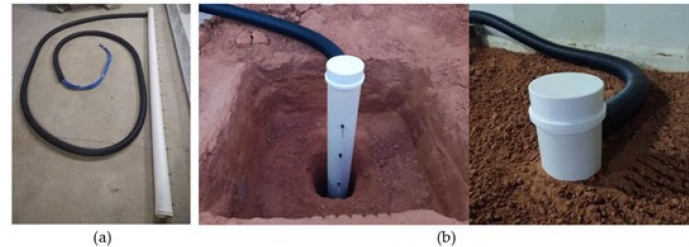

(a)   (b)

Figure 3. Measurement system installation: (**a**) attachment of the sensors to the 50-mm corrugated conduit and 100-mm PVC pipe; (**b**) PVC pipe with DS18B20 sensors inserted into the soil.

2.2. Equipment Accuracy

To ensure the highest measurement reliability, the entire data acquisition system was pre-calibrated, and its sensors were periodically checked and replaced throughout the monitoring period. Every three months, we verified the calibration and performed preventive replacements of the sensors with others that had been pre-calibrated using a certified sensor. This approach ensured continuous measurements with maximum precision.

2.3. Representativeness of the Experimental Area

The sensor installation location was carefully chosen in a region predominantly characterized by Oxisol [27]. The site exhibited typical attributes of this type of soil, including color, texture, structure, and sequence of horizons.

To confirm the soil type, soil samples were collected and analyzed in the laboratory, which verified the soil as an Oxisol. Then, samples from the 0–20 cm depth layer were analyzed, air-dried, crushed, and passed through a 2 mm sieve for grain size distribution analysis using the pipette method [32]. This allowed us to classify the soil as clay loam, determine soil bulk density by the volumetric ring method, and measure the organic carbon content through organic matter oxidation with potassium dichromate in a sulfuric medium. The results supported the typical patterns expected for Oxisols [33].

The area was isolated and located far from sources of disturbance. During the entire experimental period, vegetation control was maintained, and no anthropogenic activities occurred that could influence the characteristics of the soil under study.

The magnitude and speed of soil responses depend on its thermal properties, such as conductivity, specific heat, and thermal diffusivity, which in turn vary with texture, structure, moisture, and composition [34,35]. For example, Oxisols, with their clayey loam texture, have lower conductivity and thermal diffusivity values. Consequently, they exhibit a reduced and delayed thermal response to ambient fluctuations compared to sandy soils [36,37].

2.4. Methods for Determining Thermal Diffusivity

In this study, we used a time series of soil temperature data for the analyzed period to determine the monthly thermal diffusivity of Oxisol at depths of 5–20, 20–40, 40–60, 60–80, and 80–100 cm. Three methods were employed for this purpose: the Amplitude Method, the Arctangent Method, and the Logarithm Method. We also calculated the annual thermal diffusivity for the layer spanning 5 to 100 cm using all three methods.

Amplitude Method: Assuming a periodic surface temperature with a fundamental frequency (first harmonic) and a consistent average soil temperature across all depths, [38] proposed estimating the apparent thermal diffusivity through the direct amplitude method, as described in Equation (1):

$$\alpha = \frac{\omega}{2} \left(\frac{(Z_n - Z_1)^2}{ln(A_1/A_n)^2} \right) \tag{1}$$

in which α—apparent thermal diffusivity of the soil (m^2 s^{-1}); ω—angular frequency (rad s^{-1}); A_1 and A_n—temperature amplitudes (°C); and Z_1 and Z_n—soil depths (m).

A_1 and A_n are derived from the difference between the maximum and average annual temperatures at each depth, Z_1 and Z_n, respectively.

Assuming a periodic temperature for both the surface and deeper soil layers with the first two frequencies (first and second harmonic), the apparent thermal diffusivity can be obtained using the arctangent method [39], as shown in Equation (2):

$$\alpha = \frac{\pi(Z_n - Z_{n-1})}{2\,\omega \arctan\left(\frac{A_n}{A_{n-1}}\right)} \tag{2}$$

in which α—apparent thermal diffusivity of the soil (m^2 s^{-1}); ω—frequency angular (rad s^{-1}); A_{n-1} and A_n—temperature amplitudes (°C); and Z_{n-1} and Z_n—soil depths (m).

Logarithm Method: Using only the second harmonic [40], the apparent thermal diffusivity of the soil can be expressed by the logarithm method, as shown in Equation (3):

$$\alpha = \frac{\pi(Z_n - Z_{n-1})^2}{4\,\omega\,ln\left(\frac{A_n}{A_{n-1}}\right)} \tag{3}$$

in which α—apparent thermal diffusivity of the soil (m^2 s^{-1}); ω—frequency angular (rad s^{-1}); A_{n-1} and A_n—temperature amplitudes (°C); and Z_{n-1} and Z_n—soil depths (m).

2.4.1. Equation to Calculate Heat Wave Velocity in the Soil

From the annual thermal diffusivity, we determined the annual temperature wave propagation velocity (V) in the soil in m s^{-1}, according to Equation (4):

$$V = \sqrt{2\,\omega\,\alpha} \tag{4}$$

in which V—temperature wave propagation velocity (m s^{-1}); α—thermal diffusivity of the soil (m^2 s^{-1}); and ω—angular frequency (rad s^{-1}).

2.4.2. Equation to Calculate Damping Depth

We used the annual thermal diffusivity to calculate the annual damping depth. This is the depth at which the temperature wave amplitude drops to 1/e of its surface value, with e = 2.72 (Neperian number). This constant represents how soil temperature amplitude decreases with depth, as shown in Equation (5):

$$D_a = \sqrt{\frac{2\alpha}{\omega}} \tag{5}$$

in which D_a—damping depth (m); α—apparent thermal diffusivity of the soil (m^2 s^{-1}); and ω—angular frequency (rad s^{-1}).

2.5. Statistical Analysis

Soil temperature raw time series data were collected over 2 years, from 28 July 2020 to 27 July 2022, at 5-min intervals. This yielded 288 daily measurements (24 h $\times$ 60 min)/5 min for each depth.

To derive representative daily values, we conducted a rigorous statistical process commonly used in agricultural experiments. Potential outliers were detected and excluded using the Grubbs test [41,42]. Subsequently, we calculated the simple arithmetic mean of the valid values for each day and depth. Data normality was verified with the Shapiro-Wilk test at a 5% significance level [43]. These daily averages represent statistically robust and reliable values [44–46].

Daily averages were calculated using R 4.3.0 software. First, we used the "grubbs.test" function to detect potential outliers, which were individually examined before possible exclusion. After this, we employed the mean function to calculate the simple arithmetic mean of the remaining valid values for each day and depth. Data normality was assessed using the "shapiro.test" function.

For this study, we collected 24 months of data to compare the amplitude, arctangent, and logarithm methods used for estimating soil thermal diffusivity. Data were grouped at the end of the period to compare paired groups corresponding to each month of the year. This approach allowed for hourly average calculations and monthly result comparisons.

The analysis was conducted in the R 4.3.0 software. For the comparison of paired groups, we used the function "t.test (y1, y2, paired = TRUE) # where y1 and y2 are numerical" to perform the paired *t*-test. The corresponding months of the two years were separated and grouped to match the days and hours. The averages were calculated for each grouped day and time. Since no significant differences were found between the paired days, we then proceeded with the experimental period analyses.

We performed an analysis of variance (ANOVA) for each soil layer (5–20, 20–40, 40–60, 60–80, and 80–100 cm). Tukey's test was applied to the results with a significance level of 0.05. As noted by Ref. [47], statistical estimators help to describe the structure of spatial dependence, which is influenced by geodesic distance, sample shape, and size.

3. Results

The time series of soil temperature data, collected at depths of 5, 20, 40, 60, 80, and 100 cm, as well as ambient temperature, from 28 July 2020 to 27 July 2022, is presented in Figure 4 through paired hourly averages of year 1 with year 2.
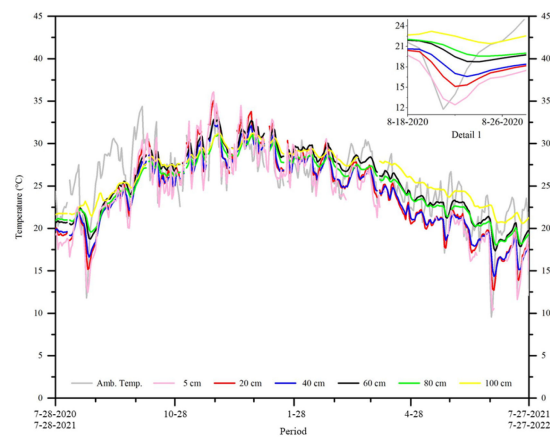
Figure 4. Paired hourly averages of soil and ambient temperatures for the studied period.

Throughout the year, soil temperatures at all depths were consistent and averaged about 25 °C. This was similar to the average ambient temperature for the Oxisol studied, as shown in Figure 5.
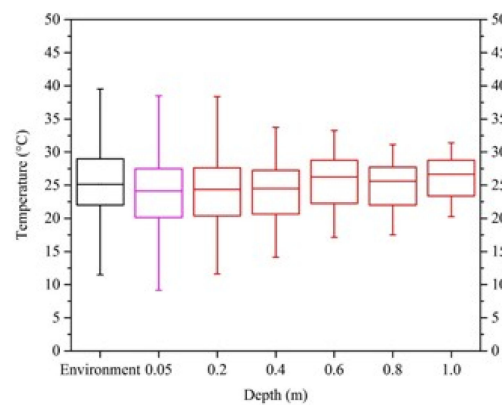
Figure 5. Boxplot of subsoil and ambient temperatures in the studied Oxisol.

Figure 6 illustrates the rapid decrease in soil thermal amplitude within the upper layers, down to a depth of 0.4 m. Beyond this depth, the reduction in thermal amplitude occurs at a slower pace.
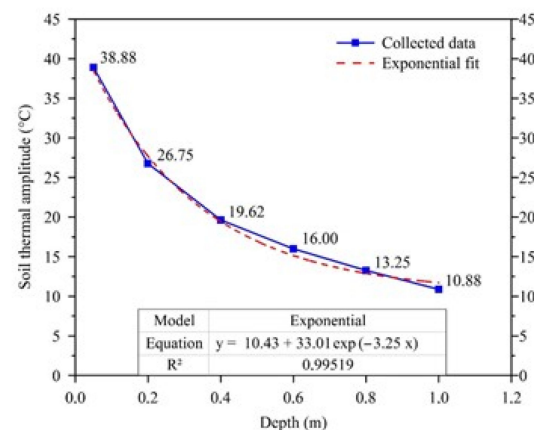
Figure 6. Annual thermal amplitude of the studied soil.

We installed temperature sensors at depths of 5, 20, 40, 60, 80, and 100 cm to analyze each of the soil layers (5–20, 20–40, 40–60, 60–80, and 80–100 cm). The thermal diffusivity

values estimated by the amplitude, arctangent, and logarithm methods showed significant differences across all layers, as shown in Figure 7 (ANOVA, $p < 0.05$).
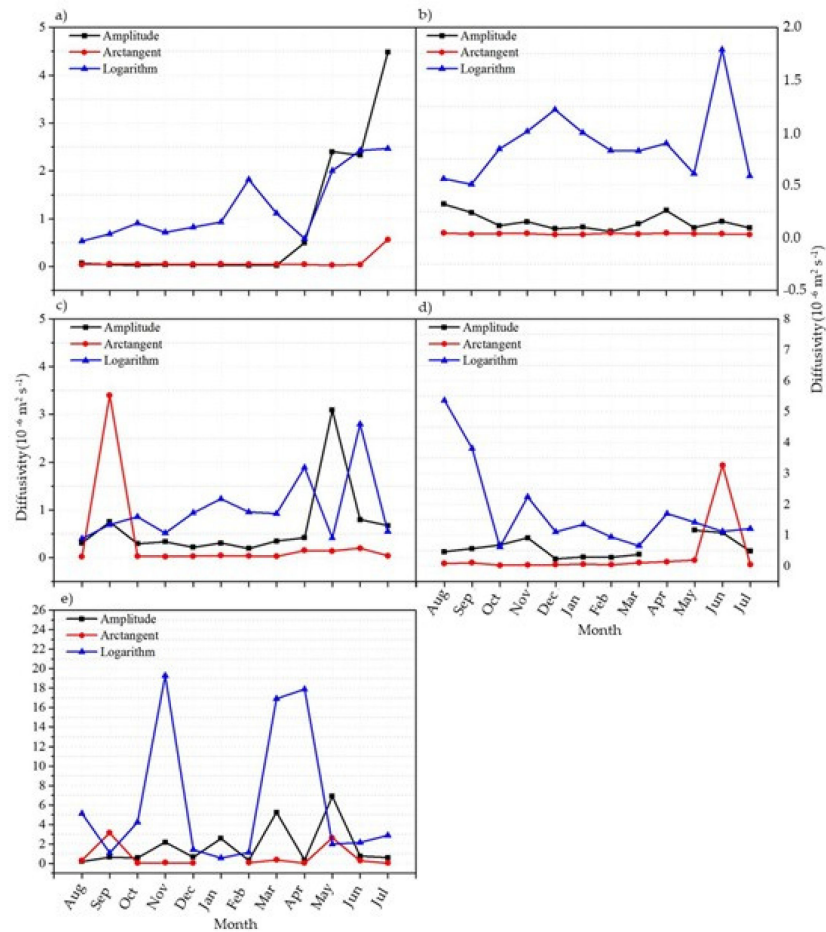

Figure 7. Monthly thermal diffusivity values for soil layers at (**a**) 5–20 cm, (**b**) 20–40 cm, (**c**) 40–60 cm, (**d**) 60–80 cm, and (**e**) 80–100 cm, as estimated by the amplitude, arctangent, and logarithm methods.

Figure 8 shows the distribution of monthly thermal diffusivity for each method used, highlighting that the logarithm method overestimated the values compared to the amplitude and arctangent methods.
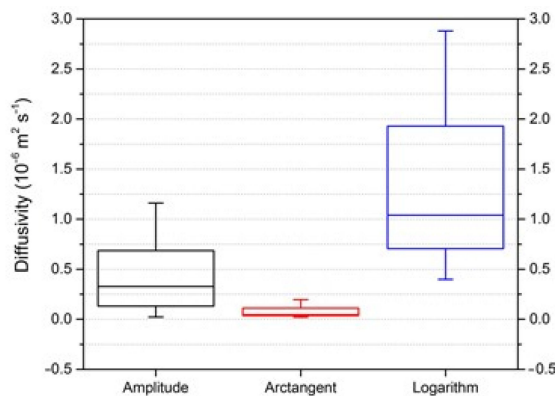

Figure 8. Boxplot of monthly soil thermal diffusivity values by amplitude, arctangent, and logarithm methods.

Table 1 displays the annual average thermal diffusivity, heat wave propagation speed, and damping depth of the Oxisol for depth layers from 0.05 to 1.00 m.

Table 1. Annual averages of thermal diffusivity, heat wave propagation velocity, and damping depth for the studied Oxisol in the layers from 0.05 to 1.00 m.

Soil Layer (m)	Thermal Diffusivity (10^{-6} m^2 s^{-1})	Propagation Velocity (10^{-6} m^2 s^{-1})	Damping Depth (m)
0.05 to 1.00	0.137	0.233	1.172

4. Discussion

The present study investigated the thermal conductivity of Oxisols using a modern technique that combines sensors, arduinos, and modules in a field experiment. The findings help to address gaps in our understanding of this soil type under in situ conditions, building on previous research conducted using other methods and experimental conditions. The ongoing development of sensors and computational techniques has significantly advanced soil thermal conductivity studies, particularly in terms of observation accuracy and spatial-temporal variability [48,49].

As shown in Figure 4, the thermal behavior of soil layers from 5 to 100 cm follows a trend similar to that of ambient temperature, exhibiting sinusoidal fluctuations throughout the year. This finding is consistent with a study conducted by [50] on red and yellow Latosols (Oxisols) in São Paulo, Brazil (22°52′30″ S, 46°22′8″ W) and another by [51] in southern Algeria (32°38′ N, 3°81′ E, 469 m altitude) on red sandy loam soil, both of which showed similar sinusoidal behavior.

Figure 4 also reveals that the soil layer at 5 cm is more sensitive to ambient temperature changes. This layer had higher temperatures between November and January compared to deeper layers, corresponding to the summer period in the study area (Brazil), which typically experiences the highest ambient temperatures. Conversely, during the winter months (June to September), the temperature of the 5 cm layer was lower than the other layers, aligning with the period of lowest ambient temperatures. Similar observations were reported in a study [52] conducted in southeastern Brazil (20°12′43″ S, 50°55′38″ W, 413 m altitude) on a red-yellow argisol soil and another study [53] that investigated soil temperature and showed a behavior similar to that found in our study. In addition to seasonality, the magnitude of ambient temperature fluctuations also affects soil heat flux. Larger thermal amplitudes intensify the soil-atmosphere thermal gradients and heat flux within the soil profile [54]. In extreme cases, such as heat waves, anomalous underground temperature responses may occur, with potential consequences for soil biota [55,56].

In the second half of August of Year 1 (Figure 4—Detail 1), a time lag in heat transfer through the soil is evident. After the minimum ambient temperature was recorded, all soil layers gradually registered minimum temperatures, with the soil layer at 100 cm requiring four days to reach its minimum temperature.

A study [57] conducted in southeastern Brazil (21°13′40″ S, 44°57′50″ W, 925 m altitude) on an Oxisol and another [58] study in Midwest Brazil (22°11′53″ S, 54°56′03″ W, 430 m altitude) that investigated heat transfer and storage in Oxisols also demonstrated a time lag in heat transfer from the topmost layer to the deepest layer. Understanding the thermal behavior of Oxisols and the dynamics of their thermal diffusivity is vital for comprehending their temperature variations.

The present study contributes to the field by enhancing our understanding of the thermal behavior of Red Oxisol and its impact on heat transfer in plants and animals in these regions. Additionally, the findings presented in Figure 4 offer insights into the thermo-hydrological processes of this soil type, which are beneficial for sustainable natural resource management across various geographical regions.

Figure 5 indicates that the soil layers at 5 and 20 cm depths exhibited the highest thermal amplitudes, with variations of 38.88 and 26.75 °C, respectively. This is attributed to their proximity to the soil surface, making them more susceptible to external temperature fluctuations. Conversely, the 100 cm layer had the lowest oscillation, with a temperature variation of only 10.88 °C throughout the year. Hence, there is a reduction in thermal

amplitude with increasing depth, demonstrating a thermal damping effect in the soil. This relationship between amplitude and depth can be characterized as inversely proportional. Similar reductions in thermal amplitude with increasing soil depth were observed in other studies [59] where the thermal behavior of Oxisols was analyzed and showed findings consistent with ours.

The observation of thermal amplitudes at varying soil depths (Figure 5) provides valuable insights into the thermal behavior of Red Oxisol and its interaction with external temperature variations. The more significant temperature oscillations in the surface layers are attributed to their proximity to the surface, making them more prone to temperature fluctuations.

Several ecological factors influence the thermal variation observed in the upper soil layers, such as incident solar radiation, the soil's thermal conductivity, and the heat exchange rate with the atmosphere [60]. Physical processes and soil properties can account for the increase in soil thermal damping with depth. The heat transfer rate diminishes with the soil depth, leading to less influence from external temperature variations [61].

This inverse relationship between thermal amplitude and soil depth, as presented in Figure 5, holds significant implications for understanding the thermal dynamics of Oxisols and their impact on ecological, hydrological, and agricultural processes. Knowledge of these thermal patterns is vital for informed decision-making regarding soil management, particularly for crops sensitive to extreme temperature variations.

Figure 6, with an R^2 of 0.99519 for the fit performed, confirms that the thermal amplitude of the soil decreases with increasing depth, exhibiting exponential behavior. According to Ref. [62] a high coefficient of determination (R^2) indicates high reliability and precision in the response of what is being observed. A recent study [63] conducted in Northeast China ($121°30'20''$ E, $50°49'40''$ N, 845 m altitude) investigated the transmission of surface temperature changes to various soil depths. The results indicated that this transmission occurs within a specific time frame and with exponentially damped amplitudes. These findings were supported by the work of [64], who proposed a reformulation of a model used for estimating soil temperature. According to these authors, the thermal amplitude of the soil exhibits an exponential variation as a function of depth, consistent with the findings of the present study.

As demonstrated in Figure 6, exploring the thermal behavior of the soil, including its exponential variation of thermal amplitude with depth, is crucial for understanding production cycles. Deepening our knowledge of the thermal behavior of soils and determining their thermal diffusivity is essential for advancing scientific knowledge, promoting sustainable practices, and managing ecosystem resources [65].

In light of these findings, it becomes evident that accounting for the exponential decrease in temperature amplitude with increasing soil depth is crucial when designing soil management strategies. Therefore, decisions related to sustainable agricultural resource use must embrace this phenomenon, especially for crops sensitive to extreme temperature fluctuations.

In a comparison of the 5–20 cm and 80–100 cm layers, the logarithmic method was found to be statistically different from the arctangent method (Figure 7). However, no significant differences were observed between the amplitude method and the others. In the 20–40 cm and 60–80 cm layers, both the amplitude and arctangent methods showed no differences, while the logarithmic method differed from both. Similar findings have been reported in other studies that utilized various models to determine soil thermal diffusivity. Research by [66] on calcareous clayey alluvial soils in eastern Turkey and by [67] in northwest Greece ($39°37'12''$ N and $20°50'24''$ E, 485 m altitude) employed amplitude, arctangent, and logarithmic models, respectively. It is noteworthy that the results from these studies are consistent with the findings of our research.

An increasing trend in the monthly thermal diffusivity of soil from April to July is evident in Figure 7. This rise is attributed to the cooler temperatures of the autumn and winter seasons, which result in higher soil moisture levels and greater soil resistance, as confirmed by [68].

A study by [69] supports this trend, reporting thermal diffusivity values for an Oxisol in Areia-PB, Brazil, ranging from 0.22×10^{-6} m^2 s^{-1} to 1.91×10^{-6} m^2 s^{-1}. However, these values narrowed to 0.22×10^{-6} m^2 s^{-1} to 0.51×10^{-6} m^2 s^{-1} when considering only the month with the lowest soil moisture. Both studies underscore the significant influence of seasonal temperature and moisture fluctuations on soil thermal diffusivity.

As illustrated in Figure 7, the colder temperatures of the autumn-winter period led to an increase in thermal resistance, which in turn limited heat flux in the soil. This results in enhanced thermal diffusivity, a parameter reflecting the soil's capacity to conduct heat and which is directly affected by changes in soil physical properties such as thermal resistance. Such changes are often influenced by seasonal climatic variations [70,71]. Gaining insight into the behavior of thermal diffusivity in Oxisol is crucial for efficient agricultural resource management and the adoption of sustainable soil management strategies. Factoring in seasonal shifts in soil thermal diffusivity is important for informed decision-making related to crop planning, energy consumption, and assessing the effects of climate on agricultural productivity.

Monthly diffusivity estimates for the studied soil ranged from 0.02×10^{-6} m^2 s^{-1} to 1.89×10^{-6} m^2 s^{-1} (Figure 8), aligning with the findings in the literature. Ref. [72] reported a range of 1512×10^{-6} m^2 s^{-1} to 2813×10^{-6} m^2 s^{-1} for an Oxisol in Garanhuns-PE, Brazil. In contrast, Ref. [73] obtained values ranging from 0.32×10^{-6} m^2 s^{-1} to 0.47×10^{-6} m^2 s^{-1} for an Oxisol in Dourados-MS, Brazil.

Understanding the thermal behavior of soil is essential for effectively managing ecological and energy resources. Figure 8 illustrates the diffusivity of the Oxisol under study, which holds particular significance due to the widespread presence of this soil type in major agricultural-producing nations such as Brazil [74]. It influences processes such as nutrient availability, seed germination, plant growth, and organic matter decomposition [75]. Thus, understanding soil diffusivity is vital for the successful management of agricultural systems' production and sustainability.

Furthermore, soil diffusivity plays a crucial role in regulating energy flow between the soil surface and the atmosphere, as well as in water conservation and climate change mitigation [76,77]. As such, knowledge of soil thermal properties, including diffusivity, is essential for optimizing agricultural production and managing ecological and energy resources sustainably.

Table 1 shows that the diffusivity values for soil layers between 0.05 and 1.00 m deep align with those reported by other researchers. Specifically, Ref. [78] found diffusivity for sandy soil in Qinghai-Tibet, China, to range from 0.117×10^{-6} m^2 s^{-1} to 0.826×10^{-6} m^2 s^{-1}. Likewise, Ref. [35] reported that soil thermal diffusivity near the surface of the Tibetan Plateau typically ranges from 0.3×10^{-6} m^2 s^{-1} to 1.9×10^{-6} m^2 s^{-1}.

The observed heat wave propagation velocity of 0.233×10^{-6} m s^{-1} is also in line with previous findings. Ref. [79] reported a propagation velocity of 0.72×10^{-6} m s^{-1} for agricultural soil. These similarities between our results and prior research support the reliability of our thermal diffusivity and heat wave propagation velocity findings.

Table 1 also indicates that the average heat-damping depth occurred at 1.172 m. However, Ref. [80] observed that sandy soils rapidly increase their damping capacity with moisture content. Consequently, multilevel monitoring of underground soil temperature is essential for accurately identifying different heat inputs based on existing sources [81]. This monitoring has enabled a deeper understanding of the soil's thermal processes, offering valuable insights into its interaction with the environment and aiding the development of sustainable environmental management strategies and responsible agricultural practices, as supported by prior studies [82,83].

The interaction between soil and atmosphere in response to environmental fluctuations hinges on both inherent pedological attributes and the nature of thermal variations. This study provides experimental data on this dynamic in Oxisols, adding to the knowledge about a soil type that is highly prevalent in tropical regions like Brazil [84–86].

In conclusion, this study on the thermal behavior of Oxisols and their thermal diffusivity highlights the importance of the characteristics explored herein given their interactions with ecological, water, plant, and animal resources, as well as soil-derived energy resources. These attributes have direct implications for food production and agricultural sustainability. However, the successful completion of this research was not without challenges. Precise soil temperature data collection at different depths was difficult due to the extended experimental duration and numerous climate fluctuations. Additionally, interpreting the results required sophisticated analyses and advanced mathematical modeling to elucidate clear relationships between the soil's thermal properties and its potential for heat transfer.

5. Conclusions

The thermal behavior of Oxisols follows a sinusoidal trend throughout the year, mirroring ambient temperature variations.

Heat transfer within the soil experiences a temporal lag, with minimum temperatures in deeper layers occurring after minimum ambient temperatures. This leads to a thermal delay between the surface and the deepest layers analyzed.

The thermal amplitude of Oxisols diminishes with increasing depth, indicative of the soil's thermal dampening effect.

The amplitude, arctangent, and logarithm methods each display significant differences, but all proved appropriate for estimating the soil's thermal diffusivity in various contexts.

The relationship between soil and environmental temperatures has substantial implications for sustainable agriculture and effective environmental monitoring.

This research sheds light on soil-environment interactions, promotes the judicious use of natural and energy resources, and provides insights for sustainable agricultural production.

Based on these findings, further research could investigate the influence of various climatic and ecological factors on soil thermal characteristics, including analysis in the context of climate change. Advanced remote sensing techniques, such as satellite and drone imagery combined with in-situ temperature and humidity measurements, could be used. This would enhance our understanding of thermoregulatory processes and offer valuable information for effective land management, natural resource conservation, and agricultural sustainability.

Conflicts of Interest: The authors declare no conflict of interest.

References

1. Pellegrina, H.S. Trade, Productivity, and the Spatial Organization of Agriculture: Evidence from Brazil. *J. Dev. Econ.* **2022**, *156*, 102816. [CrossRef]
2. de Carvalho, A.M.; de Jesus, D.R.; de Sousa, T.R.; Ramos, M.L.G.; de Figueiredo, C.C.; de Oliveira, A.D.; Marchão, R.L.; Ribeiro, F.P.; Dantas, R.d.A.; Borges, L.d.A.B. Soil Carbon Stocks and Greenhouse Gas Mitigation of Agriculture in the Brazilian Cerrado—A Review. *Plants* **2023**, *12*, 2449. [CrossRef] [PubMed]
3. Azevedo, R.P.; Silva, L.d.C.M.d.; Pereira, F.A.C.; Peche, P.M.; Pio, L.A.S.; Mancini, M.; Curi, N.; Silva, B.M. Interactions between Intrinsic Soil Properties and Deep Tillage in the Sustainable Management of Perennial Crops. *Sustainability* **2023**, *15*, 760. [CrossRef]
4. Bahry, C.A.; Fin, S.S.; Ritter, R.; Perboni, A.T.; Feliceti, M.L.; da Silva, J.A.; Carleso, Â.A. Superação da dormência de sementes de cornichão e seu efeito nos atributos fisiológicos/Dormancy overcoming of birdsfoot trefoil seeds and its effect in the physiological attributes. *Braz. J. Dev.* **2020**, *6*, 31951–31966. [CrossRef]
5. dos Santos, S.R.G.; Oliveira, R.S.S.F.; Silva, S.D.S.R. Germinação de sementes de Mabea fistulifera em diferentes substratos e temperaturas. *Res. Soc. Dev.* **2022**, *11*, e197111234309. [CrossRef]
6. Feng, Y.; Cui, N.; Hao, W.; Gao, L.; Gong, D. Estimation of Soil Temperature from Meteorological Data Using Different Machine Learning Models. *Geoderma* **2019**, *338*, 67–77. [CrossRef]
7. Seward, A.; Reeves, R.; Alcaraz, S. Assessment of the Surface Heat Loss from Waimangu Geothermal Valley: Comparison of Terrestrial Based Assessment Techniques with Remote Sensing. *J. Volcanol. Geotherm. Res.* **2022**, *430*, 107630. [CrossRef]
8. Kardani, N.; Bardhan, A.; Samui, P.; Nazem, M.; Zhou, A.; Armaghani, D.J. A Novel Technique Based on the Improved Firefly Algorithm Coupled with Extreme Learning Machine (ELM-IFF) for Predicting the Thermal Conductivity of Soil. *Eng. Comput.* **2021**, *38*, 3321–3340. [CrossRef]
9. Younes, H.; Mao, M.; Sohel Murshed, S.M.; Lou, D.; Hong, H.; Peterson, G.P. Nanofluids: Key Parameters to Enhance Thermal Conductivity and Its Applications. *Appl. Therm. Eng.* **2022**, *207*, 118202. [CrossRef]
10. Zeng, S.; Yan, Z.; Yang, J. An Improved Model for Predicting the Thermal Conductivity of Sand Based on a Grain Size Distribution Parameter. *Int. J. Heat Mass Transf.* **2023**, *207*, 124021. [CrossRef]
11. Hassan, A.M.; Belal, A.A.; Hassan, M.A.; Farag, F.M.; Mohamed, E.S. Potential of Thermal Remote Sensing Techniques in Monitoring Waterlogged Area Based on Surface Soil Moisture Retrieval. *J. Afr. Earth Sci.* **2019**, *155*, 64–74. [CrossRef]
12. da Silva, J.L.B.; Moura, G.B.d.A.; da Silva, M.V.; de Oliveira-Júnior, J.F.; Jardim, A.M.d.R.F.; Refati, D.C.; Lima, R.d.C.C.; de Carvalho, A.A.; Ferreira, M.B.; de Brito, J.I.B.; et al. Environmental Degradation of Vegetation Cover and Water Bodies in the Semiarid Region of the Brazilian Northeast via Cloud Geoprocessing Techniques Applied to Orbital Data. *J. S. Am. Earth Sci.* **2023**, *121*, 104164. [CrossRef]
13. Franco, A.; Conti, P. Clearing a Path for Ground Heat Exchange Systems: A Review on Thermal Response Test (TRT) Methods and a Geotechnical Routine Test for Estimating Soil Thermal Properties. *Energies* **2020**, *13*, 2965. [CrossRef]
14. Cai, W.; Wang, F.; Chen, C.; Chen, S.; Liu, J.; Ren, Z.; Shao, H. Long-Term Performance Evaluation for Deep Borehole Heat Exchanger Array under Different Soil Thermal Properties and System Layouts. *Energy* **2022**, *241*, 122937. [CrossRef]
15. Purdin, M.S. Determination of the Coefficient of Effective Thermal Diffusivity of Soil under Natural Changes in Environmental Conditions. *IOP Conf. Ser. Earth Environ. Sci.* **2022**, *1112*, 012034. [CrossRef]
16. Brunetti, C.; Lamb, J.; Wielandt, S.; Uhlemann, S.; Shirley, I.; McClure, P.; Dafflon, B. Probabilistic Estimation of Depth-Resolved Profiles of Soil Thermal Diffusivity from Temperature Time Series. *Earth Surf. Dyn.* **2022**, *10*, 687–704. [CrossRef]
17. Beardsmore, G.; Egan, S.; Sandiford, M. A Fourier Spectral Method to Measure the Thermal Diffusivity of Soil. *Geotech. Test. J.* **2020**, *43*, 565–587. [CrossRef]
18. Lovatto, J.; Santos, R.C.; de Souza, C.M.A.; Zucca, R.; Lovatto, F.; Geisenhoff, L.O. Use of Linear Programming for Decision Making: An Analysis of Cost, Time and Comfort of Rural Housing Dwellings. *Rev. Bras. Eng. Agríc. Ambient.* **2020**, *24*, 622–629. [CrossRef]
19. Romio, L.C.; Zimmer, T.; Bremm, T.; Buligon, L.; Herdies, D.L.; Roberti, D.R. Influence of Different Methods to Estimate the Soil Thermal Properties from Experimental Dataset. *Land* **2022**, *11*, 1960. [CrossRef]
20. Zhang, J.; Dias, D.; Pan, Q.; Ma, C.; Tsuha, C.d.H.C. Long-Term Thermo-Hydraulic Numerical Assessment of Thermo-Active Piles—A Case of Tropical Soils. *Appl. Sci.* **2022**, *12*, 7653. [CrossRef]
21. Novak, E.; Carvalho, L.A.; Santiago, E.F.; Ferreira, F.S.; Maestre, M.R. Composição química do solo em diferentes condições ambientais. *Ciênc. Florest.* **2021**, *31*, 1063–1085. [CrossRef]
22. Vergasta, L.A.; Correia, F.W.S.; Chou, S.C.; Nobre, P.; Lyra, A.d.A.; Gomes, W.d.B.; Capistrano, V.; Veiga, J.A.P. Assessment of the Water Budget in Madeira River Basin Simulated by the Eta Regional Climate and MGB Large-Scale Hydrological Models. *Rev. Bras. Meteorol.* **2021**, *36*, 153–169. [CrossRef]

23. Nunes, H.B.; Kato, E.; de Sá, M.A.C.; Rosa, V.A.; de Carvalho, A.d.S.; Soares Neto, J.P. Influência da temperatura sobre a agregação do solo avaliada por dois métodos. *Ciênc. Florest.* **2019**, *29*, 496–507. [CrossRef]

24. Silva, J.F.G.; Gonçalves, W.G.; Costa, K.A.d.P.; Neto, J.F.; de Brito, M.F.; da Silva, F.C.; Severiano, E.d.C. Crop-Livestock Integration and the Physical Resilience of a Degraded Latosol. *Semin. Ciências Agrárias* **2019**, *40*, 2973–2990. [CrossRef]

25. de Melo Benites, V.; Schaefer, C.E.G.R.; Machado, P.L.O.A.; Polidoro, J.C.; da Silva Teixeira, R. Insights into Brazilian Soils and Sustainable Agriculture Scenarios. In *The Soils of Brazil*; Schaefer, C.E.G.R., Ed.; World Soils Book Series; Springer International Publishing: Cham, Switzerland, 2023; pp. 471–486. ISBN 978-3-031-19949-3.

26. INMET. Clima e Tempo. Temperatura Média Anual. Available online: https://www.gov.br/agricultura/pt-br/assuntos/inmet/clima-e-tempo (accessed on 29 June 2023).

27. IBGE-BDIA BDIA—Banco de Dados de Informações Ambientais. Pedologia. Available online: https://bdiaweb.ibge.gov.br/#/consulta/pedologia (accessed on 29 June 2023).

28. Çuhac, C.; Mäkiranta, A.; Välisuo, P.; Hiltunen, E.; Elmusrati, M. Temperature Measurements on a Solar and Low Enthalpy Geothermal Open-Air Asphalt Surface Platform in a Cold Climate Region. *Energies* **2020**, *13*, 979. [CrossRef]

29. Sanches, Í.S.; Sanches, É.S.; Omido, A.R.; Barboza, C.S.; Jordan, R.A. Prelúdio para utilização da energia geotérmica superficial na climatização do ambiente construído na Cidade de Naviraí, Estado do Mato Grosso do Sul, Brasil. *Res. Soc. Dev.* **2020**, *9*, e4909108864. [CrossRef]

30. Agostinho, V.P.; Sanches, I.S.; Sanches, É.S.; Omido, T.V.; Barboza, C.S.; Omido, A.R. Subsídios Para Utilização Da Energia Geotérmica Superficial Na Climatização Do Ambiente Construído Em Ouro Verde—SP: Monitoramento Da Temperatura Do Subsolo Local. *Rev. Caribeña Cienc. Soc.* **2023**, *12*, 607–626. [CrossRef]

31. Cesca, R.S.; Santos, R.C.; Goes, R.H.d.T.e.B.d.; Favarim, A.P.C.; de Oliveira, M.S.G.; da Silva, N.C. Thermal Comfort of Beef Cattle in the State of Mato Grosso Do Sul, Brazil. *Ciênc. Agrotec.* **2021**, *45*, e008321. [CrossRef]

32. Pinto, L.C.; Chagas, W.F.T.; Amaral, F.H.C. Physical Attributes of a Dystroferric Red Latosol (Oxisol) under Different Management Systems. *R. Agrogeoambiental* **2019**, *11*, 111–119. [CrossRef]

33. Mangieri, V.L.; Tavares, J. Avaliação de matéria orgânica, densidade e porosidade do latossolo vermelho em contato com lixiviado de resíduos sólidos urbanos. *Eng. Sanit. Ambient.* **2019**, *24*, 1251–1258. [CrossRef]

34. Zhu, X.; Gao, Z.; Chen, T.; Wang, W.; Lu, C.; Zhang, Q. Study on the Thermophysical Properties and Influencing Factors of Regional Surface Shallow Rock and Soil in China. *Front. Earth Sci.* **2022**, *10*, 1–13. [CrossRef]

35. Tong, B.; Xu, H.; Horton, R.; Bian, L.; Guo, J. Determination of Long-Term Soil Apparent Thermal Diffusivity Using Near-Surface Soil Temperature on the Tibetan Plateau. *Remote Sens.* **2022**, *14*, 4238. [CrossRef]

36. Okorie, B.O.; Niraj, Y. Effects of Different Tillage Practices on Soil Fertility Properties: A Review. *Int. J. Agric. Environ. Res.* **2022**, *8*, 176–193. [CrossRef]

37. Pessoa, T.N.; Cooper, M.; Nunes, M.R.; Uteau, D.; Peth, S.; Vaz, C.M.P.; Libardi, P.L. 2D and 3D Techniques to Assess the Structure and Porosity of Oxisols and Their Correlations with Other Soil Properties. *CATENA* **2022**, *210*, 105899. [CrossRef]

38. Jackson, R.D.; Kirkham, D. Method of Measurement of the Real Thermal Diffusivity of Moist Soil. *Soil Sci. Soc. Am. J.* **1958**, *22*, 479–482. [CrossRef]

39. Klute, A.; Dirksen, C. Hydraulic Conductivity and Diffusivity: Laboratory Methods. In *Methods of Soil Analysis: Part 1 Physical and Mineralogical Methods*; John Wiley & Sons, Ltd.: Hoboken, NJ, USA, 1986; Volume 5, pp. 687–734. ISBN 978-0-89118-864-3.

40. Horton, R.; Wierenga, P.J.; Nielsen, D.R. Evaluation of Methods for Determining the Apparent Thermal Diffusivity of Soil Near the Surface. *Soil Sci. Soc. Am. J.* **1983**, *47*, 25–32. [CrossRef]

41. Barbato, G.; Barini, E.M.; Genta, G.; Levi, R. Features and Performance of Some Outlier Detection Methods. *J. Appl. Stat.* **2011**, *38*, 2133–2149. [CrossRef]

42. Dhekale, B.S.; Vishwajith, K.P.; Mishra, P.; Vani, G.K.; Ramesh, D. Time Series. In *Essentials of Statistics in Agricultural Sciences*; Apple Academic Press: Palm Bay, FL, USA, 2019; ISBN 978-0-429-42576-9.

43. Shapiro, S.S.; Wilk, M.B. An Analysis of Variance Test for Normality (Complete Samples). *Biometrika* **1965**, *52*, 591–611. [CrossRef]

44. Hanusz, Z.; Tarasinska, J.; Zielinski, W. Shapiro–Wilk Test with Known Mean. *REVSTAT-Stat. J.* **2016**, *14*, 89–100. [CrossRef]

45. Wei, J. The Adoption of Repeated Measurement of Variance Analysis and Shapiro—Wilk Test. *Front. Med.* **2022**, *16*, 659–660. [CrossRef] [PubMed]

46. de Souza, R.R.; Toebe, M.; Mello, A.C.; Bittencourt, K.C. Sample Size and Shapiro-Wilk Test: An Analysis for Soybean Grain Yield. *Eur. J. Agron.* **2023**, *142*, 126666. [CrossRef]

47. da Silva, N.C.; Santos, R.C.; Zucca, R.; Geisenhoff, L.O.; Cesca, R.S.; Lovatto, J. Enthalpy Thematic Map Interpolated with Spline Method for Management of Broiler Chicken Production. *Rev. Bras. Eng. Agríc. Ambient.* **2020**, *24*, 431–436. [CrossRef]

48. Kisekka, I.; Peddinti, S.R.; Kustas, W.P.; McElrone, A.J.; Bambach-Ortiz, N.; McKee, L.; Bastiaanssen, W. Spatial–Temporal Modeling of Root Zone Soil Moisture Dynamics in a Vineyard Using Machine Learning and Remote Sensing. *Irrig. Sci.* **2022**, *40*, 761–777. [CrossRef]

49. Sun, J.; Gan, W.; Chao, H.-C.; Yu, P.S. Metaverse: Survey, Applications, Security, and Opportunities. *arXiv* **2022**, arXiv:2210.07990.

50. Domingues, L.M.; de Abreu, R.C.; da Rocha, H.R. Hydrologic Impact of Climate Change in the Jaguari River in the Cantareira Reservoir System. *Water* **2022**, *14*, 1286. [CrossRef]

51. Bezari, S.; Metidji, N.; Lebbi, M.; Salem, M.; Tearnbucha, C.; Sudsutad, W.; Lorenzini, G.; Ahmad, H.; Menni, Y. Investigation and Analysis of Soil Temperature under Solar Greenhouse Conditions in a Semi-Arid Region. *Int. J. Des. Nat. Ecodynamics* **2022**, *17*, 325–332. [CrossRef]

52. Donatoni, K.A.P.; Biancho, L.E.; Aparecido, C.F.F.; de Carvalho, J.B. Temperatura do solo em áreas irrigadas com diferentes coberturas vegetais. *Unifunec Científica Multidiscip.* **2021**, *10*, 1–13. [CrossRef]

53. Diniz, J.M.T.; dos Santos, C.A.C.; da Silva, J.P.S.; da Rocha, Á.B. Reformulation of the Used Model to Estimate Soil Temperature. *Energies* **2022**, *15*, 2905. [CrossRef]

54. Oorthuis, R.; Vaunat, J.; Hürlimann, M.; Lloret, A.; Moya, J.; Puig-Polo, C.; Fraccica, A. Slope Orientation and Vegetation Effects on Soil Thermo-Hydraulic Behavior. An Experimental Study. *Sustainability* **2021**, *13*, 14. [CrossRef]

55. Brunel, C.; Farnet Da Silva, A.-M.; Lerch, T.Z.; Gros, R. Influence of Tree Residue Retention in Mediterranean Forest on Soil Microbial Communities Responses to Frequent Warming and Drying Events. *Eur. J. Soil Biol.* **2023**, *118*, 103541. [CrossRef]

56. Pugliese, G.; Ingrisch, J.; Meredith, L.K.; Pfannerstill, E.Y.; Klüpfel, T.; Meeran, K.; Byron, J.; Purser, G.; Gil-Loaiza, J.; van Haren, J.; et al. Effects of Drought and Recovery on Soil Volatile Organic Compound Fluxes in an Experimental Rainforest. *Nat. Commun.* **2023**, *14*, 5064. [CrossRef]

57. Guauque-Mellado, D.; Rodrigues, A.; Terra, M.; Mantovani, V.; Yanagi, S.; Diotto, A.; Mello, C. de Evapotranspiration under Drought Conditions: The Case Study of a Seasonally Dry Atlantic Forest. *Atmosphere* **2022**, *13*, 871. [CrossRef]

58. Sanches, É.S.; Sanches, Í.S.; Jordan, R.A.; Omido, A.R.; Motomiya, A.V.d.A.; Barboza, C.S.; Santos, R.C.; Antunes, B.M. Heat Transfer in Oxisol in Heat Storage Process. *Rev. Bras. Eng. Agríc. Ambient.* **2023**, *27*, 512–520.

59. Azevedo, R.P.; Corinto, L.M.; Peixoto, D.S.; De Figueiredo, T.; Silveira, G.C.D.; Peche, P.M.; Pio, L.A.S.; Pagliari, P.H.; Curi, N.; Silva, B.M. Deep Tillage Strategies in Perennial Crop Installation: Structural Changes in Contrasting Soil Classes. *Plants* **2022**, *11*, 2255. [CrossRef]

60. Qin, Y.; Zhang, X.; Tan, K.; Wang, J. A Review on the Influencing Factors of Pavement Surface Temperature. *Env. Sci. Pollut. Res.* **2022**, *29*, 67659–67674. [CrossRef]

61. Chung, W.J.; Park, S.H. Utilization of Thermally Activated Building System with Horizontal Ground Heat Exchanger Considering the Weather Conditions. *Energies* **2021**, *14*, 7927. [CrossRef]

62. Santos, R.C.; Lopes, A.L.N.; Sanches, A.C.; Gomes, E.P.; da Silva, E.A.S.; da Silva, J.L.B. Intelligent Automated Monitoring Integrated with Animal Production Facilities. *Eng. Agríc.* **2023**, *43*, e20220225. [CrossRef]

63. Yang, L.; Zhang, Q.; Ma, Z.; Jin, H.; Chang, X.; Marchenko, S.S.; Spektor, V.V. Seasonal Variations in Temperature Sensitivity of Soil Respiration in a Larch Forest in the Northern Daxing'an Mountains in Northeast China. *J. For. Res.* **2022**, *33*, 1061–1070. [CrossRef]

64. Léger, E.; Saintenoy, A.; Serhir, M.; Costard, F.; Grenier, C. Brief Communication: Monitoring Active Layer Dynamics Using a Lightweight Nimble Ground-Penetrating Radar System—A Laboratory Analogue Test Case. *Cryosphere* **2023**, *17*, 1271. [CrossRef]

65. Karim, A.A.; Kumar, M.; Singh, E.; Kumar, A.; Kumar, S.; Ray, A.; Dhal, N.K. Enrichment of Primary Macronutrients in Biochar for Sustainable Agriculture: A Review. *Crit. Rev. Environ. Sci. Technol.* **2022**, *52*, 1449–1490. [CrossRef]

66. Erdel, E.; Mikailsoy, F. Determination of Thermophysical Properties of Fluvisols in Eastern Turkey Using Various Models. *Eurasian Soil Sc.* **2022**, *55*, 1568–1575. [CrossRef]

67. Ioannidis, T.; Bakas, N.A. An Analytical Solution for the Heat Conduction–Convection Equation in Non-Homogeneous Soil. *Bound. Layer Meteorol* **2023**, *186*, 199–216. [CrossRef]

68. Hou, R.; Li, T.; Fu, Q.; Liu, D.; Li, M.; Zhou, Z.; Yan, J.; Zhang, S. Research on the Distribution of Soil Water, Heat, Salt and Their Response Mechanisms under Freezing Conditions. *Soil Tillage Res.* **2020**, *196*, 104486. [CrossRef]

69. Khan, M.S.; Ivoke, J.; Nobahar, M.; Amini, F. Artificial Neural Network (ANN) Based Soil Temperature Model of Highly Plastic Clay. *Geomech. Geoengin.* **2022**, *17*, 1230–1246. [CrossRef]

70. Gao, W.; Masum, S.; Qadrdan, M.; Rhys Thomas, H. A Numerical Study on Performance Efficiency of a Low-Temperature Horizontal Ground-Source Heat Pump System. *Energy Build.* **2023**, *291*, 113137. [CrossRef]

71. Suft, O.; Bertermann, D. One-Year Monitoring of a Ground Heat Exchanger Using the In Situ Thermal Response Test: An Experimental Approach on Climatic Effects. *Energies* **2022**, *15*, 9490. [CrossRef]

72. Neto, J.d.A.M.; Antonino, A.C.D.; Lima, J.R.d.S.; de Souza, E.S.; Soares, W.d.A.; Alves, E.M.; de Almeida, C.A.B.; Neto, J.A.d.S. Caracterização Térmica de Solos no Agreste Meridional do Estado de Pernambuco, Brasil (Thermal Characterization of Soils in Southern Wasteland of the State of Pernambuco, Brazil). *Rev. Bras. Geogr. Física* **2015**, *8*, 167–178. [CrossRef]

73. Omido, A.R.; Barboza, C.S.; Sanches, É.S.; Sanches, Í.S.; Omido, T.V. Subsídios Para Utilização Da Energia Geotérmica Superficial Na Climatização de Edificações: Comportamento Térmico Do Solo Latossolo Vermelho Nas Regiões Sudeste e Centro-Oeste Do Brasil. *Obs. Econ. Latinoam.* **2023**, *21*, 2672–2697. [CrossRef]

74. Silva, L.d.C.M.d.; Peixoto, D.S.; Azevedo, R.P.; Avanzi, J.C.; Dias Junior, M.d.S.; Vanella, D.; Consoli, S.; Acuña-Guzman, S.F.; Borghi, E.; de Resende, Á.V.; et al. Assessment of Soil Water Content Variability Using Electrical Resistivity Imaging in an Oxisol under Conservation Cropping Systems. *Geoderma Reg.* **2023**, *33*, e00624. [CrossRef]

75. Hartmann, M.; Six, J. Soil Structure and Microbiome Functions in Agroecosystems. *Nat. Rev. Earth Environ.* **2023**, *4*, 4–18. [CrossRef]

76. Borowski, P.F. Water and Hydropower—Challenges for the Economy and Enterprises in Times of Climate Change in Africa and Europe. *Water* **2022**, *14*, 3631. [CrossRef]

77. Chouhan, S.; Kumari, S.; Kumar, R.; Chaudhary, P.L. Climate Resilient Water Management for Sustainable Agriculture. *Int. J. Environ. Clim. Change* **2023**, *13*, 411–426. [CrossRef]

78. Dai, B.; Zhang, Y.; Ding, H.; Xu, Y.; Liu, Z. Characteristics and Prediction of the Thermal Diffusivity of Sandy Soil. *Energies* **2022**, *15*, 1524. [CrossRef]

79. Tuntrachanida, J.; Wisawapipat, W.; Aramrak, S.; Chittamart, N.; Klysubun, W.; Amonpattaratkit, P.; Duboc, O.; Wenzel, W.W. Combining Spectroscopic and Flux Measurement Techniques to Determine Solid-Phase Speciation and Solubility of Phosphorus in Agricultural Soils. *Geoderma* **2022**, *410*, 115677. [CrossRef]

80. Zhu, D.; Ciais, P.; Krinner, G.; Maignan, F.; Jornet Puig, A.; Hugelius, G. Controls of Soil Organic Matter on Soil Thermal Dynamics in the Northern High Latitudes. *Nat. Commun.* **2019**, *10*, 3172. [CrossRef]

81. Krcmar, D.; Flakova, R.; Ondrejkova, I.; Hodasova, K.; Rusnakova, D.; Zenisova, Z.; Zatlakovic, M. Assessing the Impact of a Heated Basement on Groundwater Temperatures in Bratislava, Slovakia. *Groundwater* **2020**, *58*, 406–412. [CrossRef] [PubMed]

82. Ozlu, E.; Arriaga, F.J.; Bilen, S.; Gozukara, G.; Babur, E. Carbon Footprint Management by Agricultural Practices. *Biology* **2022**, *11*, 1453. [CrossRef]

83. Sonu; Rani, G.M.; Pathania, D.; Abhimanyu; Umapathi, R.; Rustagi, S.; Huh, Y.S.; Gupta, V.K.; Kaushik, A.; Chaudhary, V. Agro-Waste to Sustainable Energy: A Green Strategy of Converting Agricultural Waste to Nano-Enabled Energy Applications. *Sci. Total Environ.* **2023**, *875*, 162667. [CrossRef] [PubMed]

84. Kazmierczak, R.; Giarola, N.F.B.; Riferte, F.B.; dos Santos, J.B.; Fogaça, A.M.; Carpinelli, S. Selection of Indicators to Discriminate Soil Tillage Systems and to Assess Soil Quality in a Red Latosol. *Braz. Arch. Biol. Technol.* **2020**, *63*, e20190489. [CrossRef]

85. Dalmolin, R.S.D.; de Araújo Pedron, F.; Curcio, G.R. Soils of the Southern Araucaria Highlands. In *The Soils of Brazil*; Schaefer, C.E.G.R., Ed.; World Soils Book Series; Springer International Publishing: Cham, Switzerland, 2023; pp. 269–297. ISBN 978-3-031-19949-3.

86. Cima, I.S.; Amaral, S.; Massi, K.G. Mapping Cerrado Remnants in an Anthropized Landscape in Southeast Brazil. *Remote Sens. Appl. Soc. Environ.* **2023**, *32*, 101032. [CrossRef]